



LAWRENCE  
LIVERMORE  
NATIONAL  
LABORATORY

# Sorption Behavior and Morphology of Plutonium in the Presence of Goethite at 25 and 80°C

M. Zavarin, P. Zhao, Z. Dai, S. A. Carroll, A. B.  
Kersting

June 15, 2012

## **Disclaimer**

---

This document was prepared as an account of work sponsored by an agency of the United States government. Neither the United States government nor Lawrence Livermore National Security, LLC, nor any of their employees makes any warranty, expressed or implied, or assumes any legal liability or responsibility for the accuracy, completeness, or usefulness of any information, apparatus, product, or process disclosed, or represents that its use would not infringe privately owned rights. Reference herein to any specific commercial product, process, or service by trade name, trademark, manufacturer, or otherwise does not necessarily constitute or imply its endorsement, recommendation, or favoring by the United States government or Lawrence Livermore National Security, LLC. The views and opinions of authors expressed herein do not necessarily state or reflect those of the United States government or Lawrence Livermore National Security, LLC, and shall not be used for advertising or product endorsement purposes.

This work performed under the auspices of the U.S. Department of Energy by Lawrence Livermore National Laboratory under Contract DE-AC52-07NA27344.

## 2. Sorption Behavior and Morphology of Plutonium in the Presence of Goethite at 25 and 80°C

Mavrik Zavarin\*, Pihong Zhao, Zurong Dai, Susan A. Carroll and Annie B. Kersting

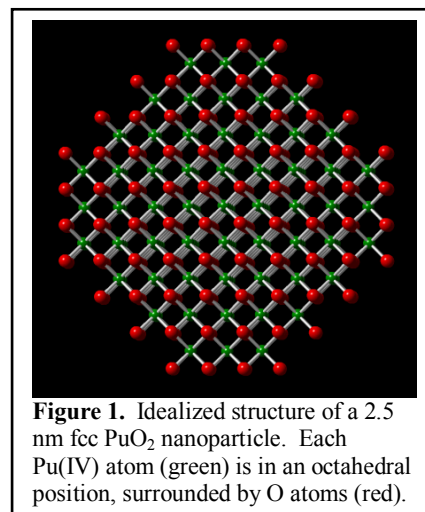
\* Glenn T. Seaborg Institute, Physical and Life Sciences Directorate, Lawrence Livermore National Laboratory, 7000 East Avenue, L-231, Livermore, California, 94551, USA

### 2.1 Introduction

Plutonium (Pu) has been identified as a dominant long-term dose contributor under certain nuclear waste repository scenarios (Kaszuba and Runde, 1999; Office of Civilian Radioactive Waste Management, 2002). The transport of Pu will likely to occur by association with natural or anthropogenic colloids or as intrinsic colloids that migrate through the engineered barrier system and host rock. The dominant anthropogenic colloids may be iron oxides produced as a result of steel corrosion (Office of Civilian Radioactive Waste Management, 2002) or intrinsic colloids formed at relatively high actinide concentrations. The mineralogy of natural colloids will be a function of the host rock mineralogy or backfill material. Host rock minerals such as smectite and iron oxide are known to sorb Pu (Bertetti et al., 1998; Keeney-Kennicutt and Morse, 1985; Kozai et al., 1996; Kozai et al., 1993; Lujaniene et al., 2007; Powell et al., 2004, 2005; Powell et al., 2008; Sabodina et al., 2006; Sanchez et al., 1985; Turner et al., 1998), which will result in actinide immobilization or retention. However, actinide sorption to these same minerals, as colloids, may also result in colloid-facilitated transport (e.g. Kersting et al. (1999)).

A major challenge in predicting the mobility and transport of actinides in the natural environment is determining the dominant geochemical processes that control their transport behavior. The reaction chemistry of Pu (*i.e.*, aqueous speciation, solubility, sorptivity, redox chemistry, and affinity for colloidal particles, both abiotic and microbially-mediated) is particularly complicated. Its migration is known to be oxidation-state dependent and facilitated by transport on particulate matter (*i.e.*, colloidal particles). Despite the recognized importance of colloid-facilitated transport, little is known about the geochemical and biochemical mechanisms controlling Pu-colloid (intrinsic or pseudo-colloid) formation and stability, particularly under relevant environmental conditions. At high concentrations ( $>10^{-9}$  M), Pu tends to form intrinsic nano-colloids (Neck et al., 2007); it is not known whether these nano-colloids are produced or are stable at very low (e.g.  $<10^{-9}$  M) concentrations. Future radioactive waste repositories will likely involve environments at elevated temperatures. Thus, the effect of elevated temperature on the stability and sorptivity of monomeric and colloidal Pu is relevant as well.

The structure of Pu precipitates and nano-colloids has been investigated for many years, particularly from the standpoint of a sol-gel processes relevant to the production of dense forms of PuO<sub>2</sub> (Lloyd and Haire, 1968). Early electron microscopy studies by Haire et al. (1971) concluded that fresh Pu(IV) precipitates are composed of nanoparticles  $<2.5$  nm in size (Figure 1). The degree of crystallinity could be increased (based on x-ray diffraction line broadening) by „aging“ the precipitates for a few hours in  $<100^{\circ}\text{C}$  water. However, the fundamental size of these nanoparticles is not affected. Importantly, these



nanoparticles were found to aggregate and were not considered stable in solution. Peptization (formation of a stable dispersion of Pu colloids in water) occurred when these precipitates were heated and reacted with  $\sim 0.2\text{M HNO}_3$ . The colloidal products of this peptization have a Pu: $\text{NO}_3$  ratio of  $\sim 1$ . Larger crystallites (4-10 nm) could be produced only upon heating ( $250^\circ\text{C}$  or greater) which also reduced the  $\text{NO}_3^-/\text{Pu}$  ratio of the colloids from  $\sim 1$  to  $\sim 0.1$  (Lloyd and Haire, 1968).

More recently, Soderholm et al. (2008) examined the structure and formation of stable colloidal suspensions of Pu precipitates in HCl/LiCl solutions. Upon evaporation from high salt solutions (2 M LiCl), a novel precipitate was formed in which  $\text{PuO}_2$ -like nano-clusters, „decorated“ by Cl anions, formed a crystalline superstructure (Figure 2). Unlike the earlier suggestions of Conradson et al. (2004), the presence of  $\text{H}_2\text{O}$  or  $\text{OH}^-$  or  $\text{Pu(V)O}_2^+$  in these nano-clusters was not identified. However, the stabilization of Pu sols in high ionic strength solutions is consistent with historical schemes developed as part of the sol-gel process. The unique scientific contribution of the Soderholm et al. (2008) work was the identification of well-ordered Pu nanoclusters that is in direct contrast to the traditional assumptions of poorly ordered polymeric or amorphous Pu(IV) precipitates. It also suggests that the  $<2.5$  nm sols produced by Haire et al. (1971) in dilute  $\text{HNO}_3$  with a Pu: $\text{NO}_3$  ratio of  $\sim 1$  may be morphologically related to these nano-clusters (Pu:Cl ratio of 0.7). However, the stability relationship between these nano-clusters and larger nano-colloids produced upon aging and heating of Pu(IV) precipitates/sols has yet to be understood.

The structure of  $\text{PuO}_2$  precipitates and colloids is complicated by the fact that Pu(IV) is susceptible to both reduction to Pu(III) and oxidation to Pu(V) and Pu(VI). Crystallographic studies of partially substituted Pu(IV) $\text{O}_2$  precipitates has been the subject of ongoing research. Conradson et al. (2004) described the structural difference between  $\text{Pu(IV)O}_2$  and  $\text{Pu(III)}_2\text{O}_3$  as an equivalent sublattice with  $\text{Pu}_2\text{O}_3$  having one of four oxygen atoms removed from the basic  $\text{PuO}_2$  fluorite structure (Figure 3). Partial removal of oxygen atoms from  $\text{Pu(IV)O}_2$  can also produce an intermediate oxidation state precipitate,  $\text{Pu}_4\text{O}_7$  (Petit et al., 2003).

A more controversial topic of ongoing research has been the structure of the partially oxidized form of  $\text{Pu(IV)O}_2$ , namely  $\text{PuO}_{2+x}$  (Conradson et al., 2004; Haschke et al., 2000; Penneman and Paffett, 2005; Petit et al., 2003). The position of the additional oxygen atoms was initially proposed to be in the octahedral vacancies in the fluorite structure. However, Conradson et al. (2004) characterized multiple preparations of  $\text{PuO}_{2+x}$  and determined that a more formal description of this phase should be  $\text{PuO}_{2+x-y}(\text{OH})_{2y} \cdot z\text{H}_2\text{O}$  in which  $\text{OH}^-$  and  $\text{H}_2\text{O}$  are structurally incorporated into the  $\text{PuO}_2$  sublattice and the oxidized Pu is most likely Pu(V) with two  $-yl$  oxygens (Figure 4). This formulation was not observed in nano-clusters characterized by Soderholm et al. (2010).

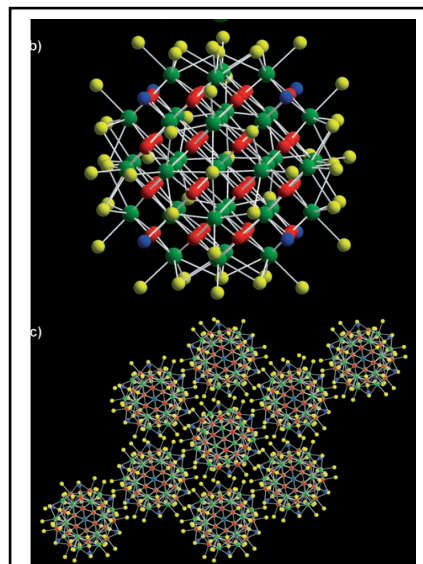


**Figure 2.** Structure and ordering of Pu(IV) nano-clusters formed in LiCl solution; the  $\text{PuO}_2$  framework exhibits a slightly distorted fcc packing of crystalline  $\text{PuO}_2$ . Each Pu(IV) atom (green) is coordinated to O (red),  $\text{H}_2\text{O}$  (blue), and/or Cl atoms that decorate the surface of the cluster (yellow). From Soderholm et al. (2010).

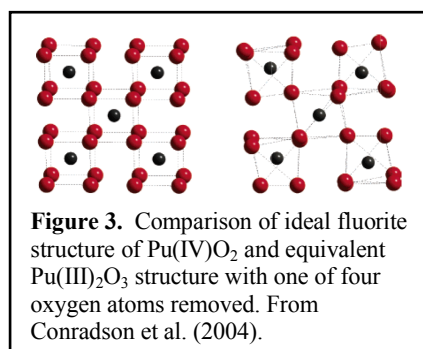
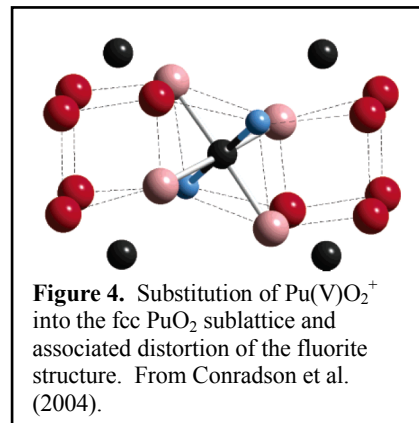


**Figure 3.** Comparison of ideal fluorite structure of  $\text{Pu(IV)O}_2$  and equivalent  $\text{Pu(III)}_2\text{O}_3$  structure with one of four oxygen atoms removed. From Conradson et al. (2004).

In their recent work, Powell et al. (2011) examined the behavior of Pu(IV) surface precipitates and colloids in the presence of goethite and quartz. Transmission electron microscopy (TEM) was used to characterize the morphology of Pu associated with these mineral phases. Plutonium was added to goethite and quartz suspensions either as „fresh“ (un-aged) Pu nano-colloids or as aqueous Pu(IV). Plutonium nano-colloids (2-5 nm) that formed on goethite from aqueous monomers underwent a lattice distortion relative to the ideal fluorite-type structure, fcc, PuO<sub>2</sub>, resulting in the formation of a bcc, Pu<sub>4</sub>O<sub>7</sub>. This structural distortion resulted from an epitaxial growth of the plutonium colloid on goethite, leading to stronger binding of plutonium compared with other minerals such as quartz where the distortion was not observed. Importantly, intrinsic PuO<sub>2</sub> nano-colloids appeared to have a weak affinity for both goethite and quartz.



The results of Powell et al. (2011) and earlier studies suggest that the morphology, structure, and stability of Pu can vary dramatically and affect the sorptivity and mobility of Pu in the environment. An understanding of the stability of Pu nano-clusters and colloids and sorption/desorption kinetics of monomeric and colloidal Pu on common minerals is critical to predicting long-term colloid-facilitated transport behavior of Pu (Cvetkovic, 2000; Cvetkovic et al., 2004; Missana et al., 2004; Saiers and Hornberger, 1996; Steefel, 2008).

In this study, we examined the sorption behavior of Pu at elevated temperatures in the presence of one relevant mineral, goethite ( $\alpha$ -FeOOH), over a range of concentrations that span solubility-controlled to adsorption-controlled concentrations. We focused on the sorptive behavior of two common forms of Pu: aqueous Pu(IV) and intrinsic Pu(IV) nano-colloids at 25 and 80°C in a dilute pH 8 NaCl/NaHCO<sub>3</sub> solution. The morphology of Pu sorbed to goethite was characterized using transmission electron microscopy (TEM). We examined the relative stability of PuO<sub>2</sub> precipitates, PuO<sub>2</sub> nano-colloids, Pu<sub>4</sub>O<sub>7</sub> surface precipitates, and monomeric sorbed Pu as a function of temperature and over a time scale of months.

## 2.2 Materials and Methods

Two series of batch sorption experiments were conducted. In the first series, aqueous Pu(IV) was reacted with goethite at 25 and 80°C. The experiment was intended to test whether the affinity or morphology of sorbed Pu was temperature dependent. The experiment was performed under identical solution conditions used in an earlier 25°C sorption isotherm experiment (0.1 g/L goethite, pH 8, 5 mM NaCl/0.7 mM NaHCO<sub>3</sub>) (Zhao et al., 2010). However, in the present case, samples were equilibrated for three months rather than two weeks. Comparison of the present data to earlier isotherm data was used to evaluate the sorption kinetics and determine the stability of surface precipitates.

In the second set of experiments, intrinsic Pu(IV) nano-colloids were reacted with goethite at 25 and 80°C. The intrinsic Pu(IV) nano-colloid sorption experiments were intended to test whether the initial form of Pu affects its longterm sorption behavior and evaluate the stability of Pu(IV) nano-colloids as a function of temperature.

At the end of the three month batch sorption experiments, Pu concentrations in the liquid phase were measured and compared to published „amorphous“ PuO<sub>2</sub> (PuO<sub>2</sub>(am, hyd)) solubility measurements (Neck et al., 2007) and sorption affinities (Zhao et al., 2010). In addition, a

detailed characterization of the Pu associated with the goethite mineral surface was conducted using TEM. The combination of liquid phase and surface characterization was used to evaluate the effect of temperature and the comparative behavior of aqueous Pu(IV) versus intrinsic nano-colloid Pu(IV) on Pu sorption characteristics.

### 2.2.1 Pu stock solution

Alpha-emitting  $^{242}\text{Pu}$  (> 99.8% by mass) was used in the experiments. The major isotopes contributing to alpha activities are  $^{238}\text{Pu}$ ,  $^{239,240}\text{Pu}$  and  $^{242}\text{Pu}$  with activity percentages of 15.9%, 5.2% and 78.9%, respectively. The Pu stock solution ( $7.6 \times 10^{-4}$  M Pu(IV) in 2.06 M HCl) was purified using AG1x8 100-200 mesh anion exchange resin and filtered through a 3kD molecular weight cut-off (MWCO) filter. The oxidation state of Pu was confirmed using both UV/VIS and solvent extraction. The aqueous Pu(IV) working solution was prepared by diluting the stock solution to  $1.9 \times 10^{-4}$  M Pu(IV) in 1N HCl. The intrinsic Pu(IV) nano-colloid working solutions were prepared by adding 1 mL 1N NaOH and 0.39 mL pH 8 buffer (5 mM NaCl/0.7 mM  $\text{NaHCO}_3$ ) to 0.53 mL of the Pu(IV) stock. Another 0.06 mL of 1N NaOH was added gradually to adjust the pH to ~8.5. The final Pu(IV) nano-colloid concentration was  $1.5 \times 10^{-4}$  and the NaCl electrolyte concentration was on the order of 1 M. The Pu(IV) nano-colloids were retained by 3kD MWCO filter. Thus, we estimate that the intrinsic nano-colloid size was generally >1 nm. Based on TEM, the fundamental particle size of intrinsic Pu nano-colloids prepared in this manner is 2-5 nm (Figure 5), somewhat larger than precipitate preparations by Haire et al. (1971) and nano-clusters of Soderhom et al. (2010). Aggregation of these intrinsic nano-colloids is commonly observed such that the aggregate size is larger (Powell et al., 2011).

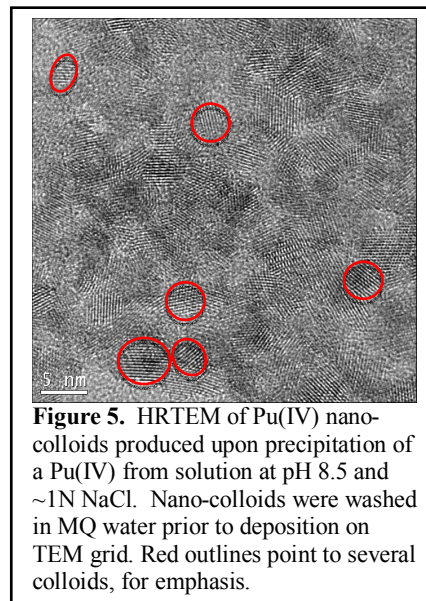


**Figure 5.** HRTEM of Pu(IV) nano-colloids produced upon precipitation of a Pu(IV) from solution at pH 8.5 and ~1N NaCl. Nano-colloids were washed in MQ water prior to deposition on TEM grid. Red outlines point to several colloids, for emphasis.

### 2.2.2 Goethite

Goethite was synthesized from  $\text{Fe}(\text{NO}_3)_3 \cdot 9\text{H}_2\text{O}$  as described by Schwertmann and Cornell (1991). Goethite was washed with a 5 mM NaCl/0.7 mM  $\text{NaHCO}_3$  buffer solution, sonicated for 5 minutes, and centrifuged for 60 minutes at 3500 rpm three times until constant pH was reached. Based on a spherical particle sedimentation estimate (Gee and Bauder, 1986), the goethite particle size retained was >100 nm. X-ray diffraction confirmed goethite as the major phase, the point of zero salt effect was  $8.5 \pm 0.1$  and the BET surface area was  $16 \text{ m}^2/\text{g}$ . The predominant morphology of the goethite particles was „star-shaped“. Additional characterization details can be found in Tinnacher et al.(2011).

### 2.2.3 Batch Experiments

All batch experiments were conducted in 10 mL Nalgene\* Oak Ridge polycarbonate centrifuge tubes with sealing caps. Either aqueous Pu(IV) or intrinsic Pu(IV) nano-colloids were spiked into 9 mL of 5 mM NaCl/0.7 mM  $\text{NaHCO}_3$  in which goethite (solid to liquid ratio of 0.1 g/L) had previously been added. Goethite-free Pu solutions were prepared in parallel. For the aqueous Pu(IV) experiments, an equivalent amount of NaOH was added before adding the Pu spike to ensure a final solution pH of 8. The 10 mL tubes were submerged in 50 mL polypropylene conical centrifuge tubes filled with MQ water to minimize evaporative losses and provide secondary containment to the radioactive samples. Over the course of the experiment, the 25°C sample tubes were stored vertically in a hood. The 80°C sample tubes were submerged in a

heated water bath. Samples were periodically shaken and weighed to check for fluid evaporative losses; no significant loss of fluid was observed over the course of the experiment.

Three initial Pu concentrations were used (Table 1) such that the resulting equilibrium Pu concentration would be below, above, and near the PuO<sub>2</sub>(am, hyd) solubility ( $\sim 5 \times 10^{-9}$  M) (Neck et al., 2007). Two goethite-free solutions (spiked blanks) with initial Pu concentrations below and above PuO<sub>2</sub>(am, hyd) solubility were used for comparison with sorption experiments. All solutions were allowed to react for 103 days.

At the conclusion of each experiment, two samples were taken from each tube. The first supernatant sample was taken after the goethite was allowed to settle out for 60 hrs. Based on sedimentation rates, we estimate that the supernatant included particles  $< \sim 250$  nm on average (Table 2). The second supernatant sample was collected after centrifugation at 5000 rpm for 90 minutes *at room temperature*. In this case, the supernatant included particles  $< \sim 25$  nm on average. Centrifugation was expected to effectively remove goethite particles. Sedimentation was also expected to remove the majority of goethite from solution. To test this, Fe in solution was monitored by ICP-MS. In all cases, Fe concentrations were low enough

such that the contribution of goethite to the measured Pu solution concentration was predicted to be negligible ( $< 0.2\%$  of Pu in solution). Neither sedimentation nor centrifugation was expected to quantitatively remove dispersed Pu(IV) nano-colloids from solution. However, centrifugation would likely remove most aggregated nano-colloids. A comparison of the sedimentation and centrifugation supernatants provides information on the presence of intermediate-sized Pu colloid aggregates in solution (25-250 nm).

#### 2.2.4 Pu analysis

Both liquid scintillation counting (LSC) and ICP-MS were used to determine Pu concentration. The LSC was used for samples with high Pu and ICP-MS used for samples in which Pu concentrations were below the LSC method detection limit ( $\sim 3 \times 10^{-10}$  M). It is important to consider the fact that sedimentation and centrifugation only segregate particles greater than the associated particle size cut off. Thus, the measured Pu concentration in solution represents both aqueous Pu and Pu nano-colloids (or aggregates) smaller than the cutoff size for sedimentation or centrifugation (i.e. Table 2).

**Table 1.** Experimental conditions for Pu(IV) samples at 25 and 80°C

Pu form	Initial Pu	Goethite conc.
	mol/L	g/L
Aqueous	$7.3 \times 10^{-11}$	0
Aqueous	$8.0 \times 10^{-7}$	0
Colloidal	$9.6 \times 10^{-11}$	0
Colloidal	$7.3 \times 10^{-7}$	0
Aqueous	$3.8 \times 10^{-9}$	0.1
Aqueous	$7.8 \times 10^{-7}$	0.1
Aqueous	$3.8 \times 10^{-6}$	0.1
Colloidal	$3.1 \times 10^{-8}$	0.1
Colloidal	$7.3 \times 10^{-7}$	0.1
Colloidal	$3.7 \times 10^{-6}$	0.1

**Table 2.** Particle segregation methods and associated particle size cut-offs.

Particle segregation method	Particle	Temp.	Particle size cut-off <sup>1</sup>
		°C	nm
Sedimentation	Goethite	25	375
Sedimentation	PuO <sub>2</sub> (am, hyd)	25	225
Sedimentation	Goethite	80	250
Sedimentation	PuO <sub>2</sub> (am, hyd)	80	125
Centrifugation	Goethite	25	35
Centrifugation	PuO <sub>2</sub> (am, hyd)	25	19

<sup>1</sup> Sedimentation rates were calculated using goethite and PuO<sub>2</sub> densities of 4.27 and 11.5 g/cm<sup>3</sup>. Fluid viscosity used at 25 and 80°C were  $8.90 \times 10^{-4}$  and  $3.55 \times 10^{-4}$ , respectively. The fluid density used at 25 and 80°C was 0.997 and 0.972 g/cm<sup>3</sup>, respectively. Sedimentation was rounded to the nearest 25 nm.

### 2.2.5 TEM Sample Preparation and Analysis

At the conclusion of each experiment, the solid phases were washed in MQ (>18 MΩ) water three times by sequentially centrifuging at 5000 rpm for 90 minutes, decanting the supernatant, and replacing it with fresh MQ water. The washing was performed to remove salts from solution. The solids were re-suspended in MQ water by sonicating for 5 minutes and diluting 10× to produce a 0.01g/L suspension. A volume of 2 to 5 uL of each suspension was deposited on TEM carbon-coated copper grids and dried in a glass desiccator. All analyses were performed on a Philips CM 300 FEG TEM operating at 300kV and equipped with a Gatan Imaging Filter (GIF) with a 2k × 2k CCD camera and an EDX detector.

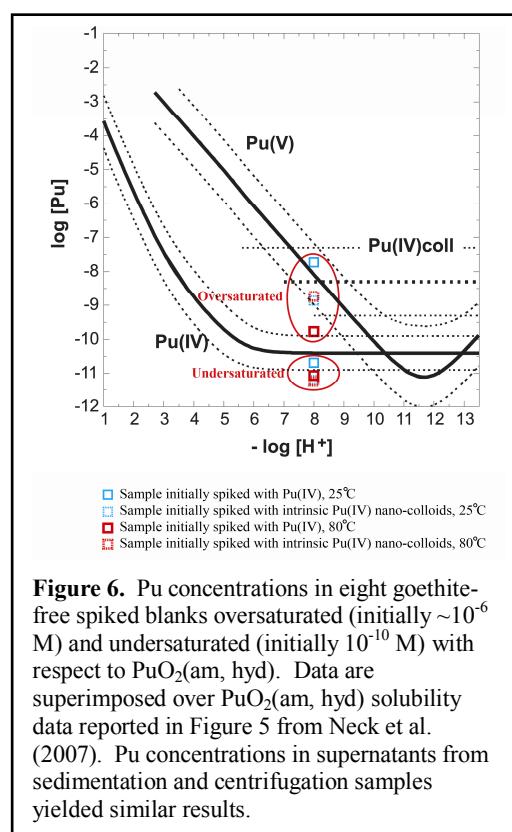
## 2.3 Results and Discussion

### 2.3.1 Pu behavior in the absence of goethite

Spiked-blanks (i.e. goethite-free solutions) were run to examine homogeneous precipitation of PuO<sub>2</sub>(am, hyd) and potential loss of Pu to container walls. Both aqueous Pu(IV) and intrinsic Pu(IV) nano-colloid solutions were equilibrated for 103 days at 25 and 80°C; initial Pu concentrations were either oversaturated (~10<sup>-6</sup> M) or undersaturated (~10<sup>-10</sup> M) with respect to PuO<sub>2</sub>(am, hyd). The solution concentration data, superimposed on the PuO<sub>2</sub>(am, hyd) solubility data presented in Neck et al. (2007), are presented in Figure 6.

For all undersaturated samples, Pu in solution was similar (sedimentation and centrifugation produced equivalent concentrations) after 103 days (~10<sup>-11</sup> M). The initial form of Pu(IV) and temperature do not appear to have an appreciable effect on Pu concentrations in solution. However, whether Pu(IV) nano-colloids dissolved or remained dispersed in solution cannot be distinguished. Significant losses of Pu from solution did occur (70-90%). We attribute these losses to sorption to container walls, as is commonly observed. Loss of Pu as a result of precipitation and/or aggregation of Pu nano-colloids is not thermodynamically favored at these concentrations.

In all high concentration (~10<sup>-6</sup> M) samples, the Pu concentration remaining in solution is consistent with the range of PuO<sub>2</sub>(am, hyd) solubility at 25°C as reported in Neck et al. (2007). Neck et al. (2007) found that a mixture of colloidal PuO<sub>2</sub> and aqueous Pu(V) are the predominant forms of Pu in solution under these conditions. However, the concentration of colloidal PuO<sub>2</sub> is conditional, depending on the choice of particle size range that is considered “colloidal”. In the case of Neck et al. (2007), the colloidal fraction was defined as the fraction collected by a 10 kD (~1.5 nm pore size) filter from a “clear supernatant”. Thus, the upper limit of the particle size considered “colloidal” is not strictly defined. In our case, the sedimentation results in a particle size upper limit estimate of ~250 nm for the solution phase. A higher upper limit would tend to increase the apparent Pu concentration in solution.



Intrinsic Pu(IV) nano-colloids “precipitated” from solution (~99.7%) in equal amounts at both temperatures. The “precipitation” is, in reality, an aging and aggregation process (Figure 5) in which PuO<sub>2</sub> nano-colloids retain their original crystallite size (2-5 nm). Importantly, these crystalline nano-colloids are larger than the nano-clusters identified by Soderholm et al. (2008) and may reflect the growth of nano-clusters to larger crystalline nano-colloids at low ionic strengths and high pH over time. The formation of Pu-Cl ionic bonding, for Pu(IV) monomers, is predicted to occur only at very low pHs (<1) where formation of hydrolysis species is not favored (Guillaumont et al., 2003). Thus, the stability of Cl-containing nano-clusters (Soderholm et al., 2008) or high NO<sub>3</sub><sup>-</sup> sols (Haire et al., 1971) is likely to be electrolyte concentration and pH dependent.

The behavior of aqueous Pu(IV) is temperature-dependent. At 103 days, the Pu concentration at 80°C was two orders of magnitude lower than at 25°C (Figure 6). Precipitation at high temperatures leads to lower apparent solubilities which reflect greater aggregation of colloidal precipitates. In contrast aggregation of pre-formed PuO<sub>2</sub> nano-colloids at high temperatures is not as effective. This implies that colloid formation and aggregation processes are irreversible. This is likely the reason why Pu(IV) colloid solubility measurements reported in Neck et al. (2007) are uncertain ( $\log K = 8.3 \pm 1.0$ ).

### 2.3.2 Pu behavior in the presence of goethite

Figure 7 presents the sorption of aqueous Pu(IV) and intrinsic Pu(IV) nano-colloids to goethite at 25°C. For each form of Pu, data at three concentrations are presented. For simplicity, we designate these as low, intermediate, and high concentration samples. For comparison, Figure 7 also includes earlier aqueous Pu(IV) isotherm data at 7 and 14 days from an experiment performed over a much wider Pu(IV) concentration range while using the identical mineral and solution conditions (Zhao et al., 2010). Solution concentration data (and associated solid concentrations) are presented based on measured Pu supernatant concentrations after sedimentation (approximately <250 nm) and centrifugation (approximately <25 nm) procedures (Table 2). Based on ICP-MS measurements of Fe in solution, goethite was effectively removed. Thus, differences between measured Pu

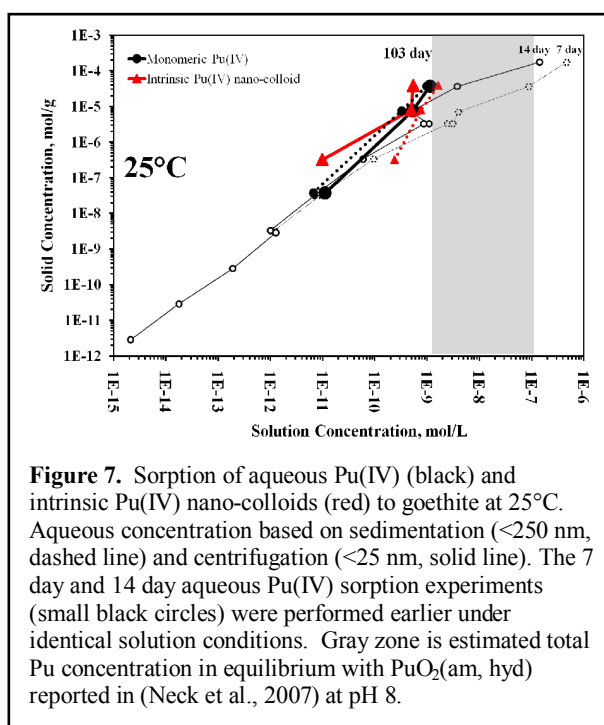


**Figure 7.** Sorption of aqueous Pu(IV) (black) and intrinsic Pu(IV) nano-colloids (red) to goethite at 25°C. Aqueous concentration based on sedimentation (<250 nm, dashed line) and centrifugation (<25 nm, solid line). The 7 day and 14 day aqueous Pu(IV) sorption experiments (small black circles) were performed earlier under identical solution conditions. Gray zone is estimated total Pu concentration in equilibrium with PuO<sub>2</sub>(am, hyd) reported in (Neck et al., 2007) at pH 8.

supernatant concentrations from these two procedures are an indication that Pu is present in substantial quantities associated with aggregated PuO<sub>2</sub> nano-particles in the 25-250 nm range.

The present aqueous Pu(IV) sorption data are in excellent agreement with the earlier isotherm data. The low concentration aqueous Pu(IV) sample matches previous data (small black symbols), indicating that equilibrium sorption was reached within 7 days. The low concentration sorption represents monomeric adsorption of Pu(IV) to the goethite surface. The intermediate concentration aqueous Pu(IV) sample matches the previous data at 14 days, indicating that sorption/surface precipitation reached equilibrium within 14 days. The highest concentration

aqueous Pu(IV) sample ( $1.1 \times 10^{-9}$  M) resulted in a solution concentration lower than the earlier 14 day sample, ( $3.8 \times 10^{-9}$  M) indicating that equilibrium had not been reached within 14 days. For the intermediate and high aqueous Pu(IV) concentration samples, solubility considerations suggest that precipitation of  $\text{PuO}_2(\text{am, hyd})$  will occur (initial Pu concentrations were  $8 \times 10^{-7}$  and  $4 \times 10^{-6}$  M, respectively, Table 1). Equilibrium solution concentrations are slightly lower than expected based on thermodynamic estimates alone (see Figure 4). However, the Pu concentration in solution may be lower simply because the particle size range to which the “colloidal” fraction was attributed ( $<250$  nm) is smaller than that used by Neck et al. (2007).

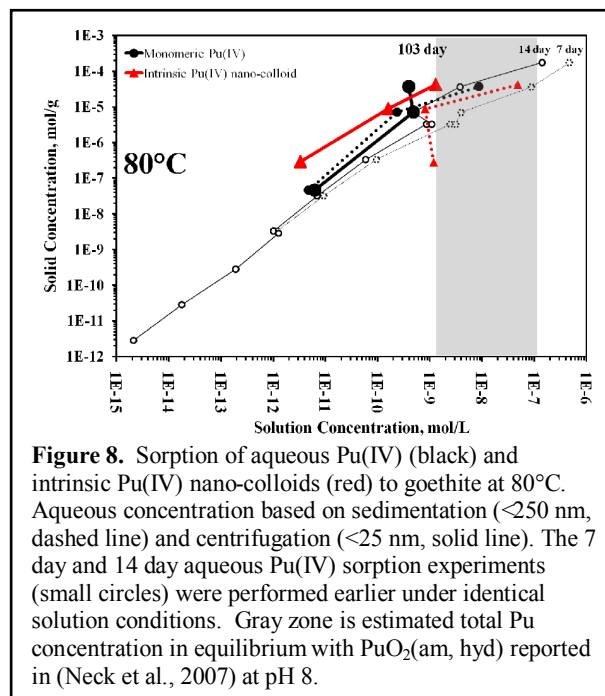
The behavior of intrinsic Pu(IV) nano-colloids differs significantly from that of aqueous Pu(IV) only in the low concentration sample. A substantial difference between Pu concentration in solution after sedimentation ( $2.4 \times 10^{-10}$  M) versus centrifugation ( $9.8 \times 10^{-12}$  M) indicates that large (25-250 nm) aggregated intrinsic Pu(IV) nano-colloids are present and do not have a strong affinity for the goethite surface. It suggests that intrinsic Pu(IV) nano-colloids at low concentrations may not be subject to sorption processes that would retard their migration. However, the intermediate and high concentration samples do not exhibit this same behavior. The intermediate and high concentration intrinsic Pu(IV) nano-colloid sorption samples result in solution concentrations similar to aqueous Pu(IV) sorption samples, driven by aggregation processes that can be categorized as precipitation.

Figure 8 presents the 80°C sorption data for aqueous Pu(IV) and intrinsic Pu(IV) nano-colloids. The 80°C aqueous Pu(IV) sorption data are similar to the 25°C data. However, greater differences in solution Pu concentrations between sedimentation and centrifugation suggest that large 25-250 nm aggregated intrinsic Pu(IV) nano-colloids may be more stable and prevalent at higher temperatures. Haire et al. (1971) also found that temperature will increase the stability of colloidal  $\text{PuO}_2$  in solution.

### 2.3.3 TEM observation of Pu morphology

#### 2.3.3.1 Aqueous Pu on goethite, 25°C

In the presence of goethite and at 25°C, aqueous Pu(IV) has been shown to grow epitaxially, forming bcc  $\text{Pu}_4\text{O}_7$  nano-colloids in the 2-5 nm particle size range (Powell et al., 2011). While previous observations were made on samples reacted for short durations, the  $\text{Pu}_4\text{O}_7$  nano-colloids appear to be stable over the longer experiment timeframe examined here (103 days). Importantly, this indicates that the  $\text{Pu}_4\text{O}_7$  is stable on the goethite surface and will not alter to a  $\text{PuO}_2$  phase over a timeframe of months.



**Figure 8.** Sorption of aqueous Pu(IV) (black) and intrinsic Pu(IV) nano-colloids (red) to goethite at 80°C. Aqueous concentration based on sedimentation ( $<250$  nm, dashed line) and centrifugation ( $<25$  nm, solid line). The 7 day and 14 day aqueous Pu(IV) sorption experiments (small circles) were performed earlier under identical solution conditions. Gray zone is estimated total Pu concentration in equilibrium with  $\text{PuO}_2(\text{am, hyd})$  reported in (Neck et al., 2007) at pH 8.

Identification of  $\text{PuO}_2$  versus  $\text{Pu}_4\text{O}_7$  on the goethite surface was accomplished by examining HRTEM FFT patterns (Figure 9).

However, we have also found that the two forms exhibit distinct morphological characteristics at the nano-scale. In general,  $\text{PuO}_2$  nano-particles form aggregates that range in size from tens to hundreds of nanometers while  $\text{Pu}_4\text{O}_7$  nano-particles are uniquely associated with the goethite surface and distributed as dispersed 2-5 nm nano-particles. These morphologies are illustrated in the following discussion.

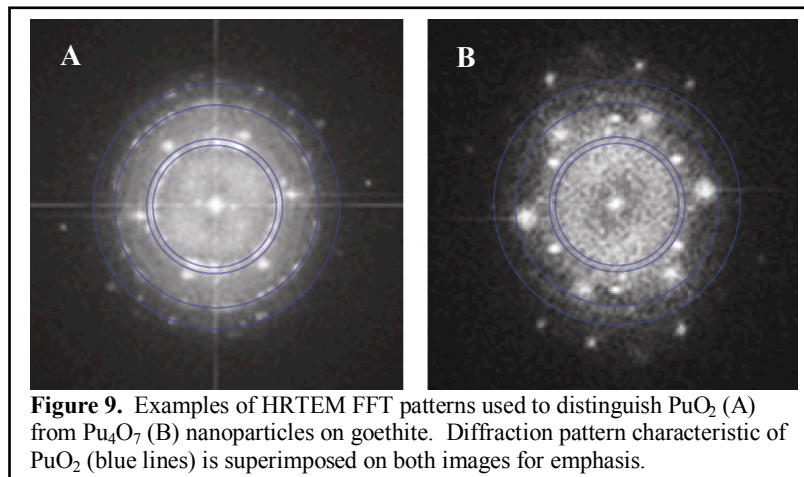


**Figure 9.** Examples of HRTEM FFT patterns used to distinguish  $\text{PuO}_2$  (A) from  $\text{Pu}_4\text{O}_7$  (B) nanoparticles on goethite. Diffraction pattern characteristic of  $\text{PuO}_2$  (blue lines) is superimposed on both images for emphasis.

In the intermediate concentration sample,  $\text{Pu}_4\text{O}_7$  nano-colloids are widely distributed over the goethite surface and dominated by isolated (dispersed) 2-5 nm nano-colloids (Figure 10). In the high concentration sample, both dispersed  $\text{Pu}_4\text{O}_7$  nano-colloids and aggregated fcc  $\text{PuO}_2$  nano-

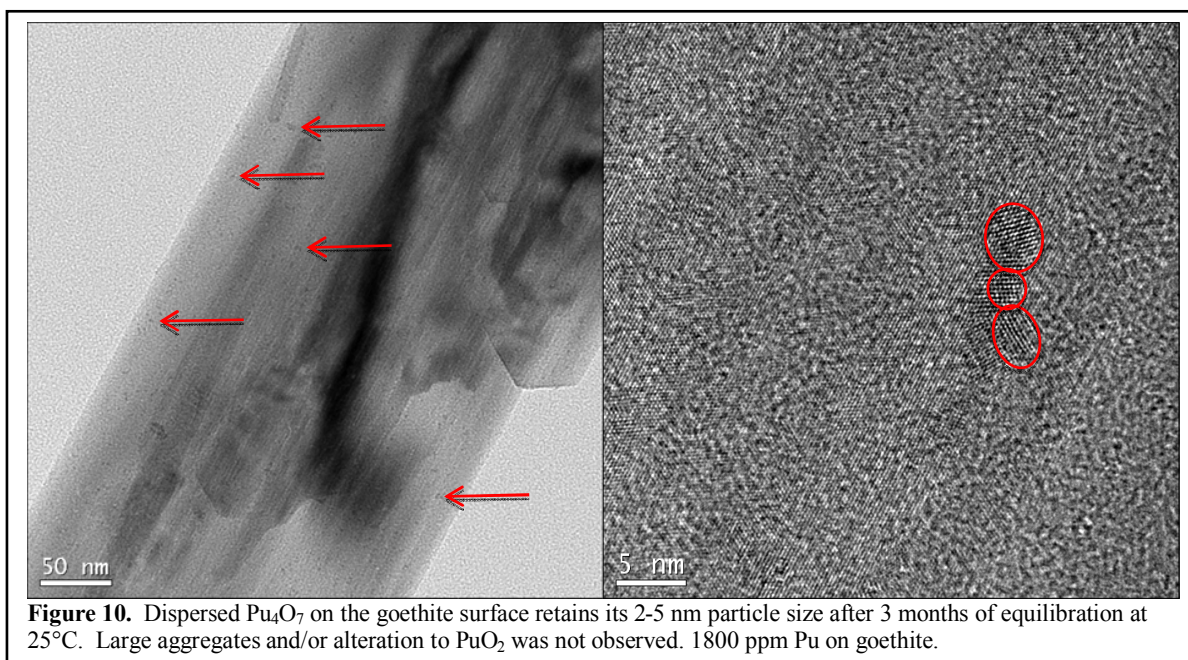


**Figure 10.** Dispersed  $\text{Pu}_4\text{O}_7$  on the goethite surface retains its 2-5 nm particle size after 3 months of equilibration at 25°C. Large aggregates and/or alteration to  $\text{PuO}_2$  was not observed. 1800 ppm Pu on goethite.

colloids exist (Figure 11). Importantly, the fundamental crystalline size remains in the 2-5 nm size range for both forms of Pu nano-colloid and in all samples. In the high concentration sample, nano-colloid aggregation is more pronounced. It cannot be ascertained whether this aggregation is purely a physical/electrostatic interaction or a chemical one. However, that difference may have a pronounced effect on the transport behavior of intrinsic Pu nano-colloids as well as the transport behavior facilitated by iron oxide colloids. Importantly, aggregated nano-colloids appear to be dominated by  $\text{PuO}_2$  nano-colloids precipitated directly from solution and weakly associated with the goethite surface. From a bulk solution standpoint, this would be

characterized as precipitation of  $\text{PuO}_2(\text{am, hyd})$ . At the nanoscale, it is characterized as aggregation of  $\text{PuO}_2$  nano-colloids.

### 2.3.3.2 Intrinsic Pu nano-colloids on goethite, 25°C

Unlike aqueous Pu(IV) sorption, intrinsic Pu(IV) nano-colloids sorption to goethite is dominated by aggregated mats of  $\text{PuO}_2$  nano-colloids. These mats were observed in both the intermediate and high concentration samples (Figure 12). The  $\text{Pu}_4\text{O}_7$  colloids that were observed in the aqueous Pu-experiments were not observed in any of the intrinsic Pu colloid experiments. Importantly, this indicates that the  $\text{PuO}_2$  colloids, once formed, will not alter to  $\text{Pu}_4\text{O}_7$  over a timeframe of months. In addition, however, the ordered  $\text{PuO}_2$  does not appear to grow beyond its initial 2-5 nm crystalline size, consistent with previous work (Haire et al., 1971).

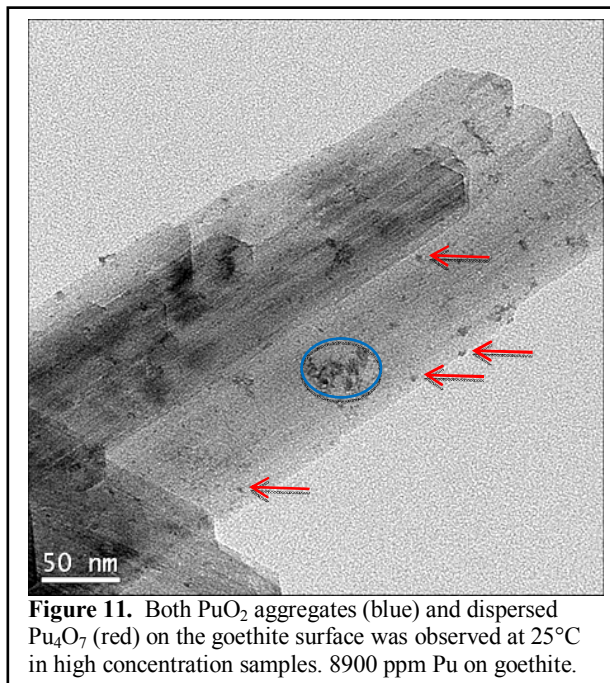


**Figure 11.** Both  $\text{PuO}_2$  aggregates (blue) and dispersed  $\text{Pu}_4\text{O}_7$  (red) on the goethite surface was observed at 25°C in high concentration samples. 8900 ppm Pu on goethite.

Because these mats are located both on and off goethite (Figure 12B and C), it is clear that the interaction between intrinsic  $\text{PuO}_2$  nano-colloids and the goethite surface is much weaker than in the case of aqueous Pu(IV) sorption. The bulk solution chemistry data (Figure 3) suggest that the same weak interaction between  $\text{PuO}_2$  nano-colloids and goethite exist at the low Pu concentration. However, identification of  $\text{PuO}_2$  colloids by TEM at low surface loading is exceedingly difficult (the needle in the haystack problem). It was not attempted for the low concentration sample.

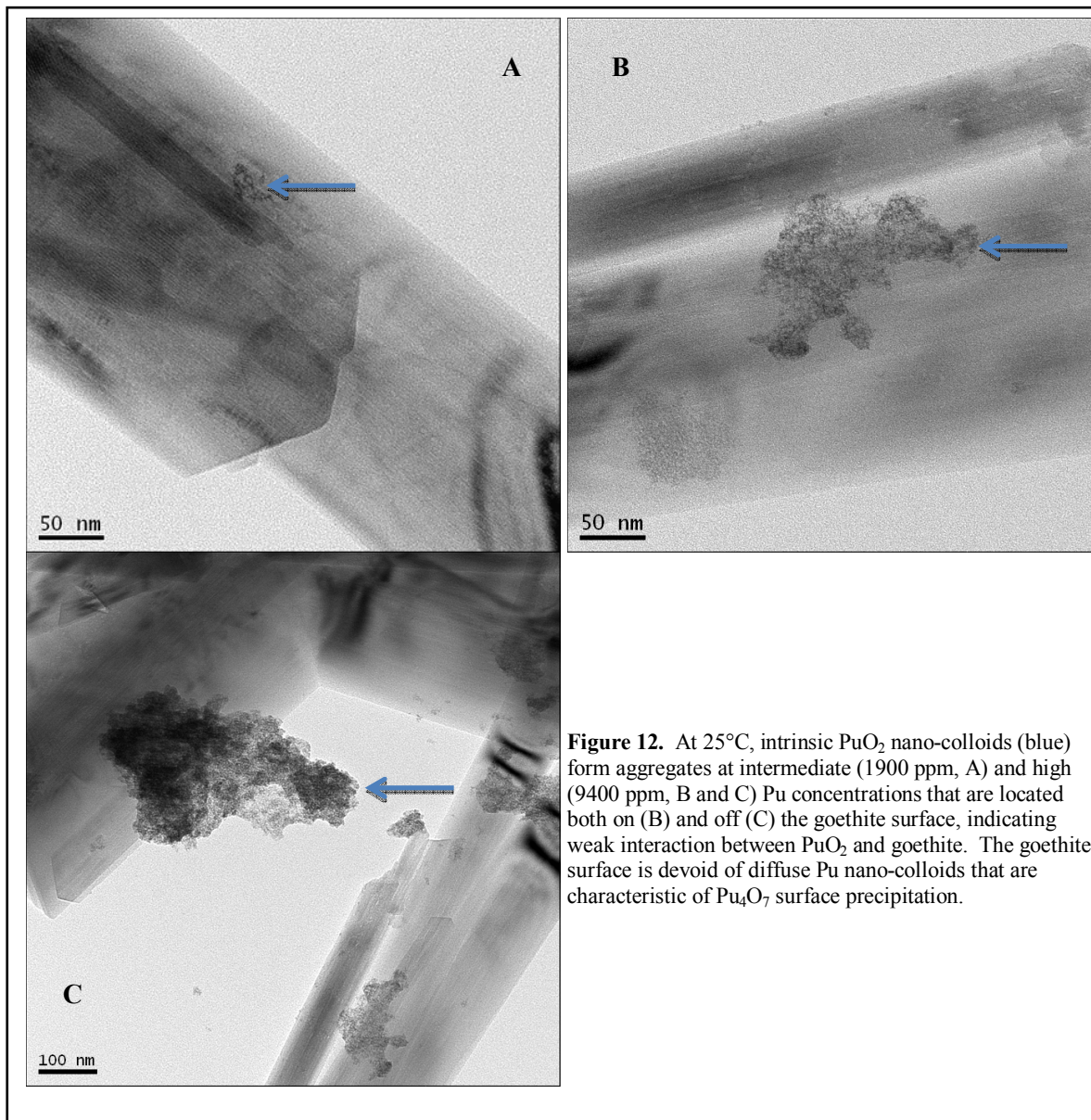


**Figure 12.** At 25°C, intrinsic  $\text{PuO}_2$  nano-colloids (blue) form aggregates at intermediate (1900 ppm, A) and high (9400 ppm, B and C) Pu concentrations that are located both on (B) and off (C) the goethite surface, indicating weak interaction between  $\text{PuO}_2$  and goethite. The goethite surface is devoid of diffuse Pu nano-colloids that are characteristic of  $\text{Pu}_4\text{O}_7$  surface precipitation.

### 2.3.3.3 Aqueous Pu on goethite, 80°C

The characteristics of Pu associated with goethite at 80°C are not substantially different from those at 25°C. The intermediate concentration aqueous Pu(IV) sample is dominated by dispersed  $\text{Pu}_4\text{O}_7$  nano-colloids that are in the 2-5 nm size range (Figure 13). In the high concentration sample, both aggregated  $\text{PuO}_2$  nano-colloids and dispersed  $\text{Pu}_4\text{O}_7$  nano-colloids are present. The aggregated  $\text{PuO}_2$  nano-colloids are located both on and off the goethite surface while the  $\text{Pu}_4\text{O}_7$  nano-colloids are strictly associated with the goethite surface. At 80°C, the size of the aggregated  $\text{PuO}_2$  nano-colloids appears to be larger. This is consistent with Pu concentrations measured in solution (Figure 5) which suggest a significant fraction of intrinsic Pu(IV) nano-colloids are aggregated and in the 25-250 nm particle size range.

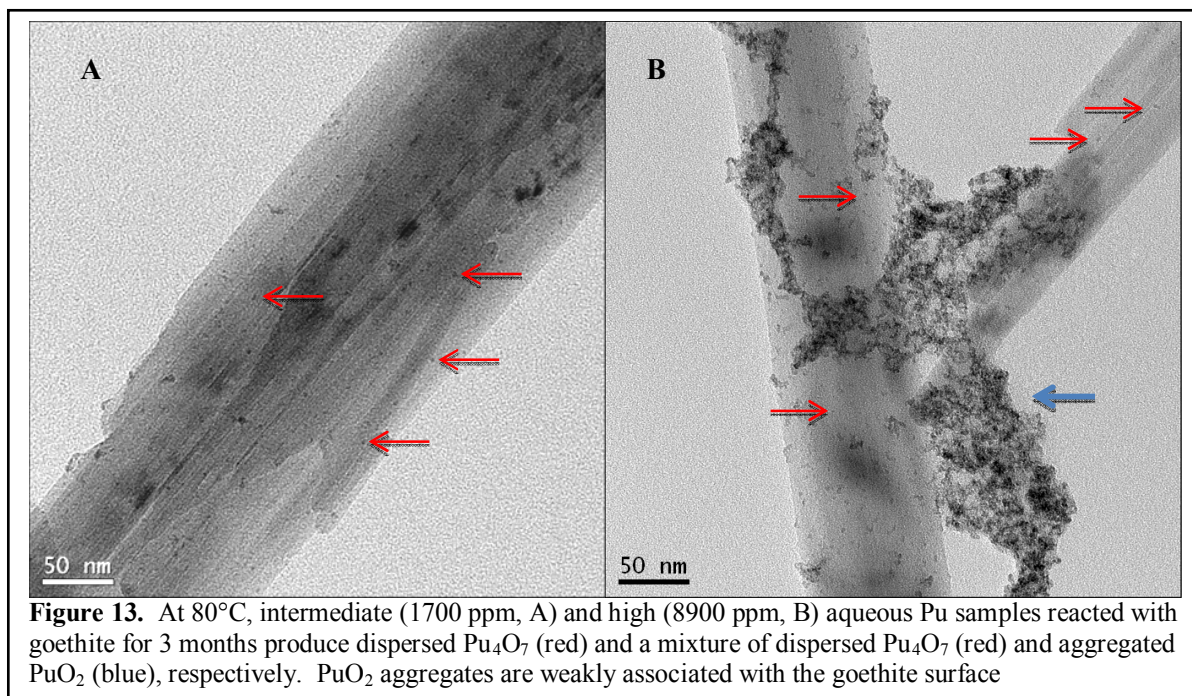


**Figure 13.** At 80°C, intermediate (1700 ppm, A) and high (8900 ppm, B) aqueous Pu samples reacted with goethite for 3 months produce dispersed  $\text{Pu}_4\text{O}_7$  (red) and a mixture of dispersed  $\text{Pu}_4\text{O}_7$  (red) and aggregated  $\text{PuO}_2$  (blue), respectively.  $\text{PuO}_2$  aggregates are weakly associated with the goethite surface

#### 2.3.3.4 Intrinsic Pu nano-colloids on goethite, 80°C

The behavior of intrinsic Pu(IV) nano-colloids at 80°C is dominated in both intermediate and high concentration samples by the formation of large aggregated  $\text{PuO}_2$  nano-colloids and little if any association with the goethite surface (Figures 14). In terms of bulk solution chemistry, these would be considered precipitates of  $\text{PuO}_2(\text{am, hyd})$ . HRTEM images and electron diffraction analysis indicate that the mats are composed of 2-5 nm nano-colloids with a fcc  $\text{PuO}_2$  structure. Importantly, the results suggest that the relationship between colloidal and precipitated forms of  $\text{PuO}_2(\text{am, hyd})$  is controlled by degree of aggregation of 2-5 nm nano-colloids. Aggregation of nano-colloids is controlled primarily by the solution conditions in which they are present (Pu concentration, solution composition (e.g. ionic strength, pH) and temperature). Thus, the concentration of dispersed intrinsic  $\text{PuO}_2$  nano-colloids in solution will most likely be controlled by the physical aggregation behavior of  $\text{PuO}_2$  nano-colloids.

#### 2.4 Conclusions

The strong affinity of aqueous Pu(IV) for the goethite surface is explained by the epitaxial growth of bcc  $\text{Pu}_4\text{O}_7$  nano-colloids on goethite. The behavior is affected minimally by temperature. However, the dispersed 2-5 nm  $\text{Pu}_4\text{O}_7$  on the goethite surface appears to be stable over the timescale of months at both 25 and 80°C. There is no indication that the  $\text{Pu}_4\text{O}_7$  alters to a more stable  $\text{PuO}_2$  nano-colloid over time. When intrinsic  $\text{PuO}_2$  nano-colloids are reacted with goethite over 103 days, both solution phase characterization in low concentration samples and TEM of high concentration samples indicate that the  $\text{PuO}_2$  nano-colloids have a very weak affinity for the goethite surface. Importantly, there is no indication that the  $\text{PuO}_2$  will alter to a more stable  $\text{Pu}_4\text{O}_7$  nano-colloid on the goethite surface over time. Thus it appears that the association of Pu to goethite is dependent on the initial state of Pu in solution.

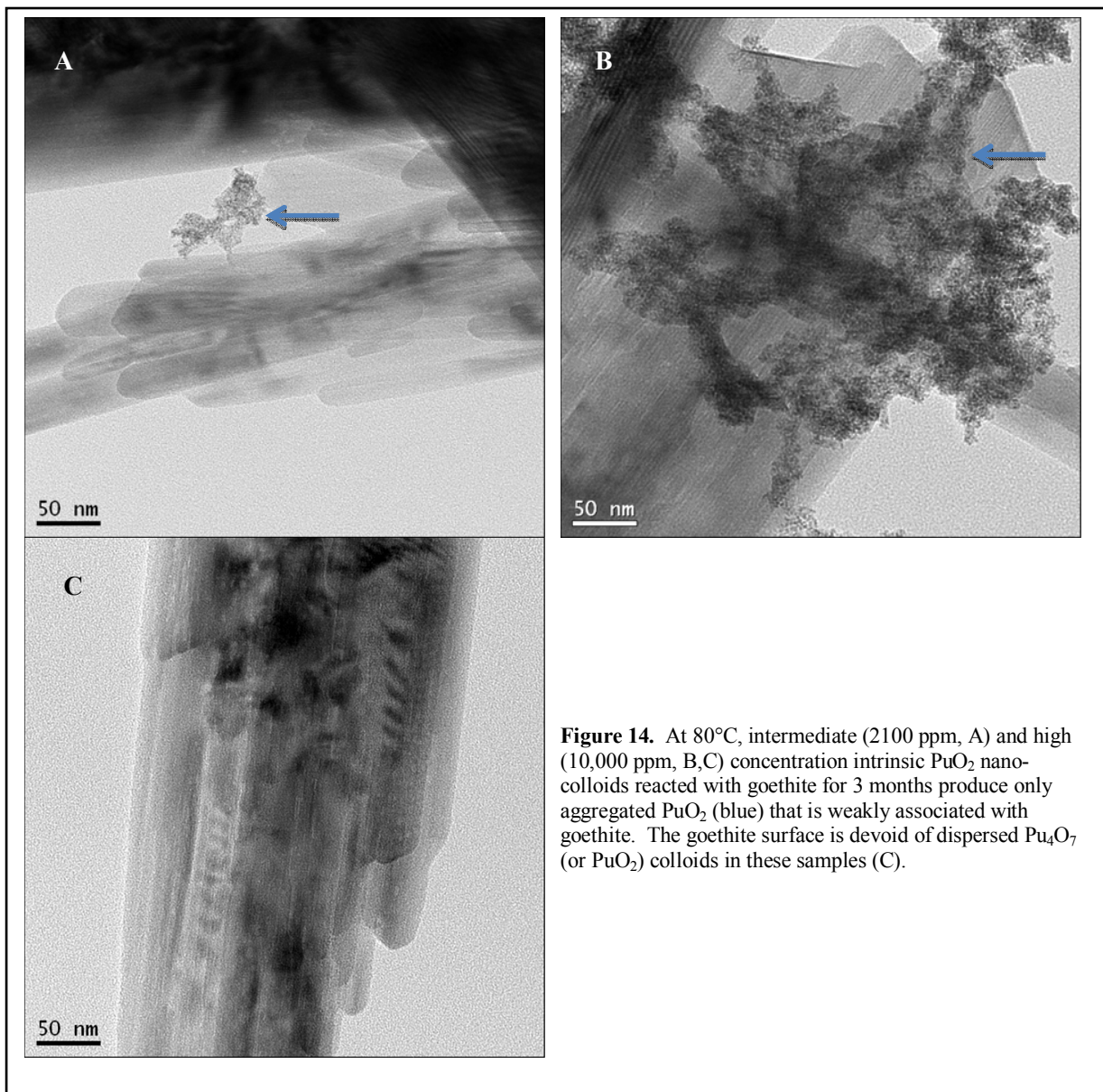


**Figure 14.** At 80°C, intermediate (2100 ppm, A) and high (10,000 ppm, B,C) concentration intrinsic  $\text{PuO}_2$  nano-colloids reacted with goethite for 3 months produce only aggregated  $\text{PuO}_2$  (blue) that is weakly associated with goethite. The goethite surface is devoid of dispersed  $\text{Pu}_4\text{O}_7$  (or  $\text{PuO}_2$ ) colloids in these samples (C).

The crystallite size of  $\text{PuO}_2$  nano-colloids is in the 2-5 nm range and appears to increase only slightly at higher temperatures and over time, consistent with earlier characterization of plutonium sols performed by Haire et al. (1971). Aggregation of  $\text{PuO}_2$  nano-colloids is favored over sorption to goethite. From a bulk solution perspective, this would be characterized as precipitation and is in agreement with solubility measurements of Neck et al. (2007) for  $\text{PuO}_2(\text{am}, \text{hyd})$ . Importantly, a truly amorphous precipitate does not form. The nano-clusters identified in Soderholm et al. (2007) represent the lower limit of colloid sizes observed here by TEM. However, the exact relationship and relative stability of nano-clusters to the larger nano-colloids observed here requires further study. In addition, the relationship between these TEM observations and the bulk characterization of Pu precipitates with apparent mixed valence (i.e.  $\text{PuO}_{2+x}$ ) remains an open question.

The fate of Pu in the environment is dependent on its initial form and its subsequent stability under changing geochemical conditions. Epitaxial growth of  $\text{Pu}_4\text{O}_7$  on the goethite surface will

produce a strong association between Pu and goethite, which could lead to its immobilization. However, the weak affinity and stability of intrinsic Pu colloids in solution and strong and irreversible formation of Pu<sub>4</sub>O<sub>7</sub> on goethite have the potential to facilitate the transport of Pu in solution facilitated by colloids.

The focus of ongoing research is on Pu nanoparticle dissolution kinetics of Pu nanoparticles and sorbed species from the iron hydroxide. Pu nanoparticle dissolution and Pu desorption kinetics must be quantified as these rates are likely to control the colloid-facilitated transport of Pu in the near-field and far-field repository environments. Experimental data summarized in this chapter illustrate the complex reaction chemistry that will control kinetics and the need for a comprehensive conceptual understanding of the underlying mechanisms controlling Pu reactive transport.

## 2.5 Acknowledgements

This work was performed with funding from the Department of Energy, Nuclear Energy Used Fuel Disposition Program. This work performed under the auspices of the U.S. Department of Energy by Lawrence Livermore National Laboratory under Contract DE-AC52-07NA27344.

## 2.6 References

- Bertetti, F.P., Pabalan, R.T., Almendarez, M.G., 1998. Studies on neptunium(V) sorption on quartz, clinoptilolite, montmorillonite, and  $\alpha$ -alumina, in: Jenne, E.A. (Ed.), Adsorption of Metals by Geomedia. Academic Press, San Diego, pp. 131-148.
- Conradson, S.D., Begg, B.D., Clark, D.L., den Auwer, C., Ding, M., Dorhout, P.K., Espinosa-Faller, F.J., Gordon, P.M., Haire, R.G., Hess, N.J., Hess, R.J., Keogh, D.W., Morales, L.A., Neu, M.P., Paviet-Hartmann, P., Runde, W., Tait, C.D., Veris, D.K., Villeda, P.M., 2004. Local and nanoscale structure and speciation in the PuO<sub>2+x-y</sub>(OH)<sub>2y</sub>·zH<sub>2</sub>O system. *J. Amer. Chem. Soc.* 126, 13443-13458.
- Cvetkovic, V., 2000. Colloid-facilitated tracer transport by steady random ground-water flow. *Physics of Fluids* 12, 2279-2294.
- Cvetkovic, V., Painter, S., Turner, D., Pickett, D., Bertetti, P., 2004. Parameter and model sensitivities for colloid-facilitated radionuclide transport on the field scale. *Water Resources Research* 40.
- Gee, G.W., Bauder, J.W., 1986. Particle-size Analysis, in: Klute, A. (Ed.), *Methods of Soil Analysis: Part I - Physical and Mineralogical Methods*. American Society of Agronomy, Inc, Madison, WI, pp. 383-411.
- Guillaumont, R., Fanghanel, T., Neck, V., Fuger, J., Palmer, D.A., Grenthe, I., Rand, M.H., 2003. Update on the Chemical Thermodynamics of Uranium, Neptunium, Plutonium, Americium, and Technetium, in: Agency, O.N.E. (Ed.), *Chemical Thermodynamics*. Elsevier, Amsterdam.
- Haire, R.G., Lloyd, M.H., Beasley, M.L., Milligan, W.O., 1971. Aging of hydrous plutonium dioxide. *Journal of Electron Microscopy* 20, 8-16.
- Haschke, J.M., Allen, T.H., Morales, L.A., 2000. Reaction of plutonium dioxide with water: Formation and properties of PuO<sub>2+x</sub>. *Science* 287, 285-287.
- Kaszuba, J.P., Runde, W.H., 1999. The aqueous geochemistry of neptunium: Dynamic control of soluble concentrations with applications to nuclear waste disposal. *Environmental Science & Technology* 33, 4427-4433.
- Keeney-Kennicutt, W.L., Morse, J.W., 1985. The redox chemistry of Pu(V)O<sub>2</sub><sup>+</sup> interaction with common mineral surfaces in dilute solutions and seawater. *Geochimica et Cosmochimica Acta* 49, 2577-2588.
- Kersting, A.B., Efurud, D.W., Finnegan, D.L., Rokop, D.J., Smith, D.K., Thompson, J.L., 1999. Migration of plutonium in ground water at the Nevada Test Site. *Nature* 397, 56-59.

- Kozai, N., Ohnuko, T., Matsumoto, J., Banba, T., Ito, Y., 1996. A study of the specific sorption of neptunium(V) on smectite in low pH solution. *Radiochim. Acta* 75, 149-158.
- Kozai, N., Ohnuky, T., Muraoka, S., 1993. Sorption characteristics of neptunium by sodium-smectite. *J. Nuclear Sci. Tech.* 30, 1153-1159.
- Lloyd, M.H., Haire, R.G., 1968. A sol-gel process for preparing dense forms of PuO<sub>2</sub>. *Nuclear Applications* 5, 114-122.
- Lujaniene, G., Motiejunas, S., Sapolaite, J., 2007. Sorption of Cs, Pu and Am on clay minerals. *Journal of Radioanalytical and Nuclear Chemistry* 274, 345-353.
- Missana, T., Garcia-Gutierrez, M., Alonso, U., 2004. Kinetics and irreversibility of cesium and uranium sorption onto bentonite colloids in a deep granitic environment. *Applied Clay Science* 26, 137-150.
- Neck, V., Altmaier, M., Seibert, A., Yun, J.I., Marquardt, C.M., Fanghanel, T., 2007. Solubility and redox reactions of Pu(IV) hydrous oxide: Evidence for the formation of PuO<sub>2+x</sub>(s, hyd). *Radiochimica Acta* 95, 193-207.
- Office of Civilian Radioactive Waste Management, 2002. Yucca Mountain Science and Engineering Report: Technical Information Supporting Site Recommendation Consideration. U.S. Department of Energy, pp. Page 4-466.
- Penneman, R.A., Paffett, M.T., 2005. An alternative structure of Pu<sub>4</sub>O<sub>9</sub> ("PuO<sub>2.25</sub>") incorporating interstitial hydroxyl rather than oxide. *J. Solid State Chem.* 178, 563-566.
- Petit, L., Svane, A., Szotek, Z., Temmerman, W.M., 2003. First-principles calculations of PuO<sub>2+x</sub>. *Science* 301, 498-501.
- Powell, B.A., Dai, Z., Zavarin, M., Zhao, P., Kersting, A.B., 2011. Stabilization of Plutonium Nano-Colloids by Epitaxial Distortion on Mineral Surfaces. *Environmental Science & Technology* 45, 2698-2703.
- Powell, B.A., Fjeld, R.A., Kaplan, D.I., Coates, J.T., Serkiz, S.M., 2004. Pu(V)O<sub>2</sub><sup>+</sup> adsorption and reduction by synthetic magnetite (Fe<sub>3</sub>O<sub>4</sub>). *Environmental Science & Technology* 38, 6016-6024.
- Powell, B.A., Fjeld, R.A., Kaplan, D.I., Coates, J.T., Serkiz, S.M., 2005. Pu(V)O<sub>2</sub><sup>+</sup> adsorption and reduction by synthetic hematite and goethite. *Environmental Science & Technology* 39, 2107-2114.
- Powell, B.A., Kersting, A.B., Zavarin, M., 2008. Sorption and Desorption Rates of Neptunium and Plutonium on Goethite, in: Zavarin, M., Kersting, A.B., Lindvall, R.E., Rose, T.P. (Eds.), *Hydrologic Resources Management Program and Underground Test Area Project, FY 2006 Progress Report*. Lawrence Livermore National Laboratory, Livermore, CA, pp. 90, UCRL-TR-404620.
- Sabodina, M.N., Kalmykov, S.N., Sapozhnikov, Y.A., Zkharova, E.V., 2006. Neptunium, plutonium and <sup>137</sup>Cs sorption by bentonite clays and their speciation in pore waters. *J. Radioanal. Nucl. Chem.* 270, 349-355.
- Saiers, J.E., Hornberger, G.M., 1996. The role of colloidal kaolinite in the transport of cesium through laboratory sand columns. *Water Resources Research* 32, 33-41.
- Sanchez, A.L., Murray, J.W., Sibley, T.H., 1985. The adsorption of plutonium IV and V on goethite. *Geochimica et Cosmochimica Acta* 49, 2297-2307.
- Schwertmann, U., Cornell, R., M., 1991. *Iron oxides in the laboratory: preparation and characterization*. VCH Verlagsgesellschaft mbH, Weinheim.
- Soderholm, L., Almond, P.M., Skanthakumar, S., Wilson, R.E., Burns, P.C., 2008. The structure of the plutonium oxide nanocluster [Pu<sub>38</sub>O<sub>56</sub>Cl<sub>154</sub>(H<sub>2</sub>O)<sub>8</sub>](14-). *Angewandte Chemie-International Edition* 47, 298-302.
- Steeffel, C.I., 2008. Geochemical kinetics and transport, in: Brantley, S.L., Kubicki, J.D., White, A.F. (Eds.), *Kinetics of Water-Rock Interaction*. Springer, New York, pp. 545-585.

- Tinnacher, R.M., Zavarin, M., Powell, B.A., Kersting, A.B., 2011. Kinetics of neptunium(V) sorption and desorption on goethite: An experimental and modeling study. *Geochimica Et Cosmochimica Acta* 75, 6584-6599.
- Turner, D.R., Pabalan, R.T., Bertetti, F.P., 1998. Neptunium(V) sorption on montmorillonite: An experimental and surface complexation modeling study. *Clays and Clay Minerals* 46, 256-269.
- Zhao, P., Zavarin, M., Tumeay, S., Williams, R., Dai, Z., Kips, R., Kersting, A.B., 2010. Isotherm of Pu/Goethite System: Linearity and Sorbent Surface Characterization, AGU Fall Meeting, San Francisco.